Numerical estimation of concrete beams reinforced with FRP bars

Kostiantyn Protchenko[1,*], *Krystian* Młodzik[2], *Marek* Urbański[1], *Elżbieta* Szmigiera[1] and *Andrzej* Garbacz[1]

[1]Warsaw University of Technology, Department of Civil Engineering, Al. Armii Ludowej 16, 00-637 Warsaw, Poland
[2]MK Projekt – Construction and Design Office, Plac Wolności 12, 46-100 Namysłów, Poland; KGE LLC, ul. Krokwi 32/25, 03-114 Warsaw, Poland

Abstract. This paper introduces numerical investigation on mechanical performance of a concrete beam reinforced with Fibre Reinforced Polymer (FRP) bars, which can be competitive alternative to steel bars for enhancing concrete structures. The objective of this work is being identified as elaborating of reliable numerical model for predicting strength capacity of structural elements with implementation of Finite Element Analysis (FEA). The numerical model is based on experimental study prepared for the beams, which were reinforced with Basalt FRP (BFRP) bars and steel bars (for comparison). The results obtained for the beams reinforced with steel bars are found to be in close agreement with the experimental results. However, the beams reinforced with BFRP bars in experimental programme demonstrated higher bearing capacity than those reinforced with steel bars, which is not in a good convergence with numerical results. Authors did attempt to describe the reasons on achieving experimentally higher bearing capacity of beams reinforced with BFRP bars.

1 Introduction

In occasion, design service life of structures is drastically affected by highly corrosive environment. The corrosion of steel bars is a material problem rather than structural one. Instead of using common practices to eliminate corrosion, more durable materials can be used.

The premise of fibre reinforced polymer FRP composites lies in their high-strength, lightweight, noncorrosive, nonconducting, and nonmagnetic properties. In addition, FRP manufacturing, using various cross-sectional shapes and material combination, offers unique opportunities for the development of shapes and forms that would be difficult or impossible with conventional steel materials [1]. The widespread implementation of FRP as a reinforcement for reinforced concrete elements requires: a comprehensive understanding of how each of these materials behaves alone as well as the behavior of the complete structural system [2].

* Corresponding author: k.protchenko@il.pw.edu.pl

In a certain circumstances, using of FRP bars can be considered as the substitute material to conventional steel in concrete detailing. If FRP is utilized as the internal reinforcement for concrete structures, it can provide high specific strength compared to the steel reinforcement [3, 4].

Current situation on the market shows that using of FRP will be confined to applications where their unique characteristics will be the most appropriate. Exist common practice to use FRP bars in a range of structural applications, such as: prestressed concrete structures, foundations, road surfaces, parking, and bridges.

The selection of the fibres is primarily based on consideration of characteristics on strength, stiffness, durability, and cost. Nevertheless, BFRP bars characterised as a new variety of material which mechanical properties are not completely investigated.

2 Mechanical Behaviour of the FRP Bar

Mechanical properties of the bar are mostly characterised by properties of their constituents i.e. fibres and matrices (described in the Figure 1). Fibres can be characterized as continuous, non-intersecting, directionalised, non-metallic and fire resistant. Basalt fibres have a longitudinal/transverse modulus ratio close to 1. Epoxy resin has viscoelastic properties and it is assumed to use it as a polymer matrix. According to test results in [5] FRP bars with epoxy resin demonstrated better physical and mechanical characteristics and lowest degradation rate after conditioning in alkaline solution than bars with other tested types of matrices.

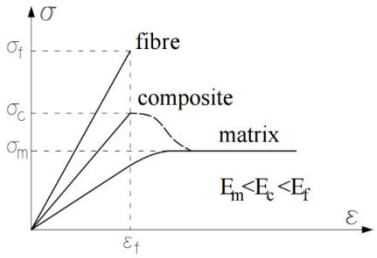

Fig. 1. Stress-strain behaviour of constituents and composite materials.

The BFRP bar can be produced in different arrangements of fibres, which then are bounded intimately in polymer matrix. Configuration of fibres defines the number of material` constants, and for the BFRP bars is assumed as hexagonal one, which can be related to the case of transverse isotropy. Detailed mechanical parameters of different bar constituents are described in [6, 7, 8, 9].

It is verified from the experimental data that for the analysis of FRP properties in the longitudinal direction (direction of fibres) the Voigt Model can be used [10, 11, 12] and for the transverse direction (perpendicular direction to direction of fibres) semi-empirical models, such as Halpin-Tsai model, which takes into account experimental data regarding bond behaviour between fibres and matrices, can be used [12].

3 The Experimental Programme

The experimental tests were performed in the laboratory of Warsaw University of Technology and described in detail in [13]. An experimental programme consisted of six beams made of concrete class *C30/37* with the dimension of $b \times h \times L = 80 \times 140 \times 1200$ *mm*, which were subjected to flexural tests. Figure 2 shows the beam structure. The actual average strength of concrete was tested on cubic samples - $f_{ck,cube} = 41.02$ *MPa*. Three of

them were reinforced at the bottom with BFRP bars of *8 mm* diameter. For comparison, three reference RC beams with bottom steel reinforcement of the same diameter were prepared. Modulus of elasticity of basalt bars was determined based on experimental data E_f=*39,05GPa* [5] and Modulus of elasticity for steel bars was assumed as *200 GPa.*

The support regions of the beams were reinforced at top by two steel bars of *8 mm* diameter and steel stirrups, however the middle part of beams were without stirrups and top reinforcement. In the beams, which were reinforced with BFRP bars, the central bottom basalt bar was made to protrude on both ends to enable the measurement of the slip in the process of loading. Clear cover were assumed as *20 mm*. The 7 pairs of bench-marks, with spacing *20 mm*, were arranged on the side surface of the beam. Registration of concrete strains was made with a mechanical extensometer with a measuring length of *100 mm.*

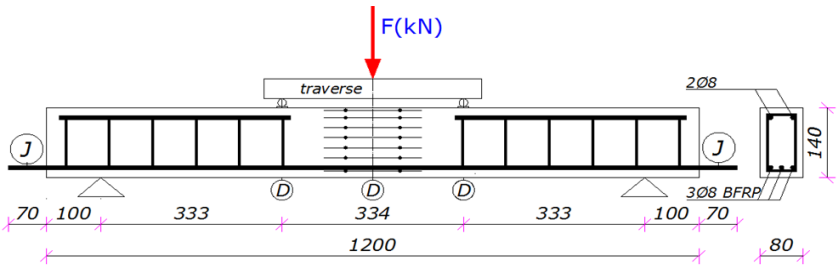

Fig. 2. The structure of tested beams with BFRP reinforcement at the bottom, J - slip measurement sensor, D - deflection gauge, dimensions in mm [13].

Loading was placed in the four point system made of steel traverse, respectively in the third and two thirds on the beam span. Loading was performed in several cycles. During the first cycle of loading, the beams were subjected to load equal to *10 kN* and then the load was reduced to *5 kN*. In each following cycle loading was increased by *10 kN*, and then reduced again to *5 kN*, till the failure of the structure.

Table 1 describes the deflections in the mid-span depending on the level of loading.

Table 1. Deformational characteristics of tested beams obtained during the experiments [13].

Applied force, kN	**Deflections, mm**					
	SRC1	SRC2	SRC3	BFRP1	BFRP2	BFRP3
5	0.97	1.81	1.61	3.21	3.04	3.10
10	1.71	2.23	2.06	4.35	4.11	4.23
20	2.45	3.30	3.14	7.33	6.99	7.21
30	3.48	4.43	4.24	12.63	11.58	12.01
40	-	-	-	-*	19.54	19.03

*The failure of the beam due to shear

Experimental results show that beams reinforced with BFRP bars have greater deflections than beams, which are reinforced with steel bars. That is mainly because the BFRP bars have significantly lower modulus of elasticity.

The Figure 3 shows the final phase of the beam "BFRP3" with the load F_U=*45 kN*. It is noteworthy that there was no rupture of the flexural basalt bars, and therefore they have not reached tensile strength. The destruction of beam took place only by shear in support zone and it had brittle nature.

Fig. 3. The destruction phase of the beam reinforced with BFRP (BFRP3) [13].

Table 2 describes the flexural capacity for beams with different reinforcement, namely SRC for the beams with steel reinforcement at the bottom, BFRP for the beams reinforced with BFRP bars at the bottom.

Table 2. Beam flexural capacity achieved with BFRP bars (BFRP) and steel bars (SRC) [13].

Parameters	Steel reinforced beams			BFRP reinforced beam		
	SRC1	SRC2	SRC3	BFRP1	BFRP2	BFRP3
F_u, kN	37.5	35.0	40.5	47.5	47.5	45.0
$F_{u,ave}$, kN	37.6			46,7		
ε_1 , ‰	-1.58	-2.17	-2.02	-1.78	-2.60	-3.25
ε_1 , ‰	4.18	5.69	6.52	9.43	13.60	7.76
$M_{R,fl}$, kNm	6.3	5.8	6.8	7.9	7,9	7.5
$M_{R,fl,ave}$, kNm	6.3			7.8		

4 The Numerical Model

Figure 4 represents the FEA model, which was performed in the Abaqus/CAE Software. The materials, which were used for the model are the same as in the experimental programme. FEA model for the concrete beam was designed by the use of grid, which consist of *660 elements* of *C3D8R* type. For the modelling of linear objects, such as: BFRP bars, steel bars and stirrups *300 elements* were used of *T3D2 type*.

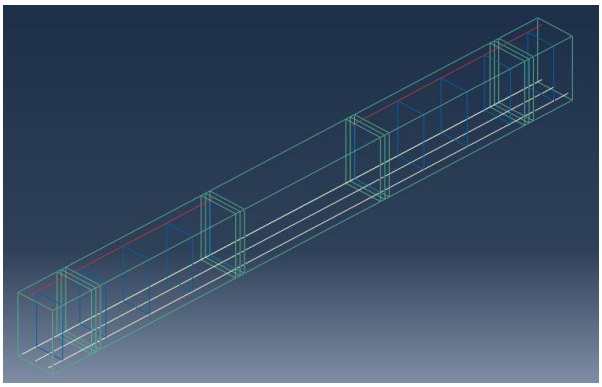

Fig. 4. The FEA model of tested beam.

Figure 5 shows the placing of the loading, which was applied in the same manner as in the experimental tests, in the form of strips with the sizes *2.0 cm* and *width of the beam*.

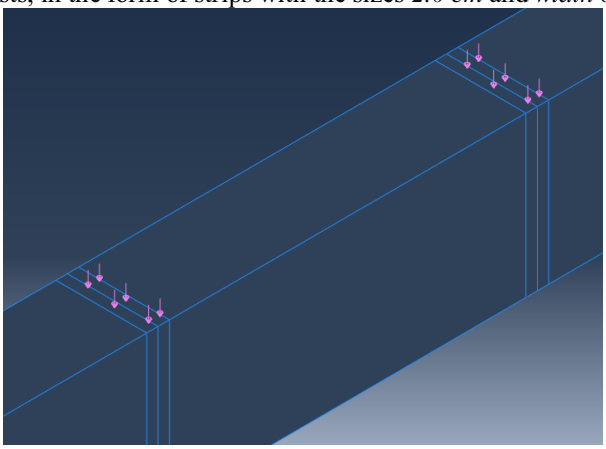

Fig. 5. The placing of loading.

The non-linear model was used with the gradual accumulation, $S=0.002$, and the beam was planned to load force, $F_{u,pl} = 20\ MN/m2$. Assuming the load transfer by the strip with dimensions, $b \times h = 0.02 \times 0.08\ m$, the final applied loading for the point force was defined according to expression 1:

$$F = F_{u,pl} \times b \times h = 20.00 \times 0.02 \times 0.08 = 32.00\ kN \quad (1)$$

The total force which was planned to apply to the beam is equal to twice the point force, which corresponds to the value of *64.00 kN*. This value exceeds the average strength obtained from experimental tests by about *37%*.

The Figure 6 shows that the program stops computation, when the element is subjected to *0.336* of the planned force. At this point, the element is destroyed.

Step	Increment	Att	Severe Discon Iter	Equil Iter	Total Iter	Total Time/Freq	Step Time/LPF	Time/LPF Inc
1	165	1	0	2	2	0.33	0.33	0.002
1	166	1	0	1	1	0.332	0.332	0.002
1	167	1	0	1	1	0.334	0.334	0.002
1	168	1	0	1	1	0.336	0.336	0.002
1	169	1	0	6	6	0.336	0.336	0.002

Fig. 6. The applying of loading at the moment of element failure.

Obtained strength, $F_{u,FEA}$, of the element is defined according to expression 2:

$$F_{u,\ FEA} = S \times F = 0.336 \times 64 = 21.50\ kN \quad (2)$$

Figure 7 and Figure 8 show distribution of stresses in the concrete and in BFRP bars, respectively, just before the destruction of the element.

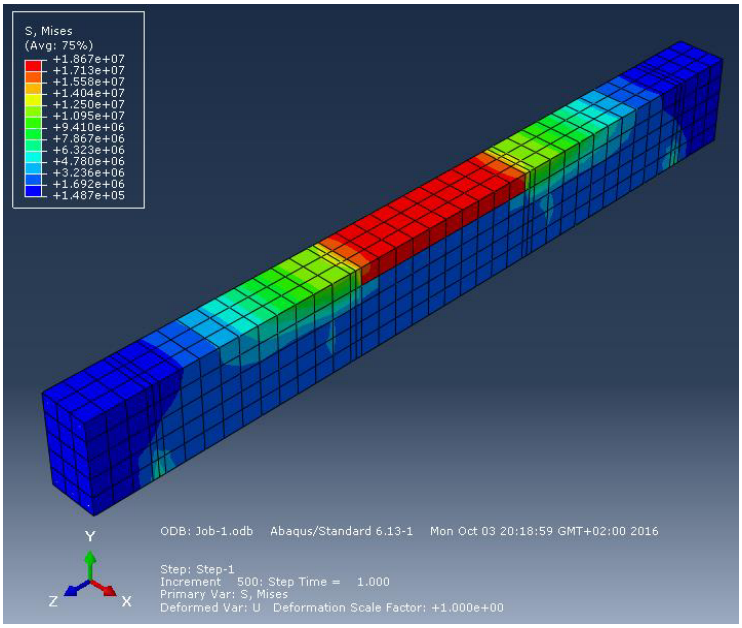

Fig. 7. Distribution of stresses in concrete element, units in Pa.

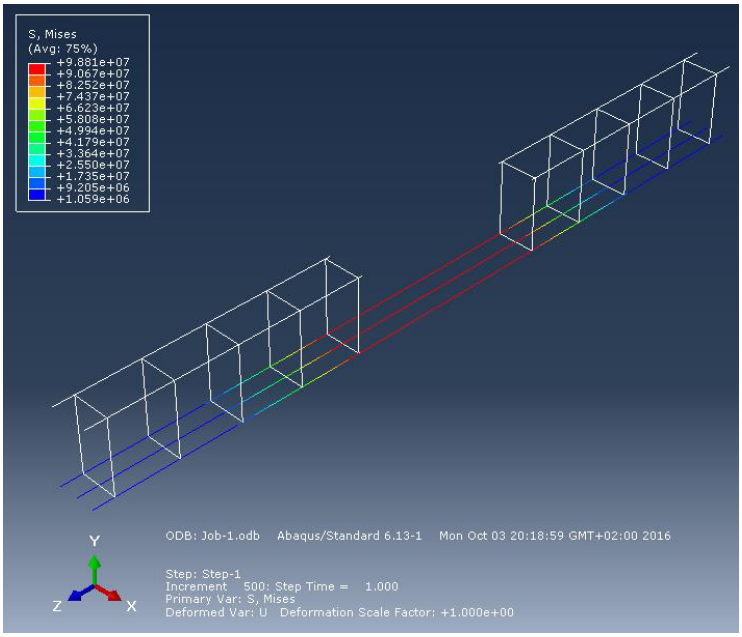

Fig. 8. Distribution of stresses in FRP reinforcement, units in Pa.

Figure 9 describes the distribution of strains for the whole element.

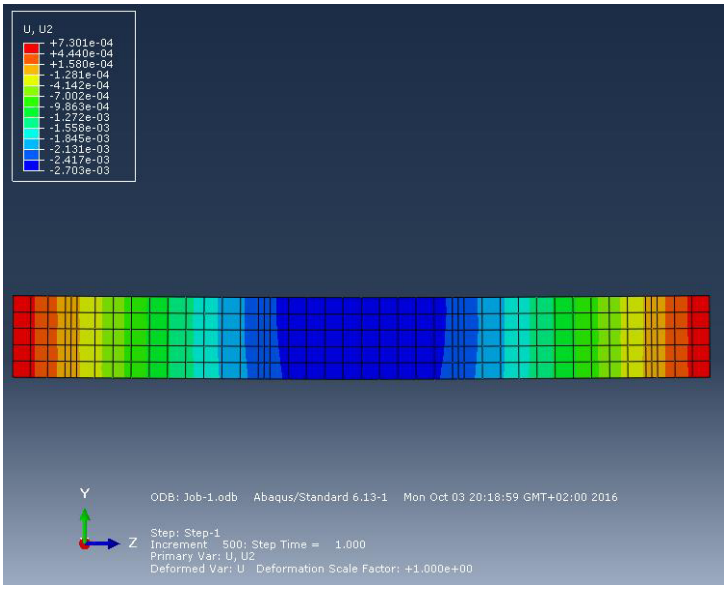

Fig. 9. Distribution of strains in the element, units in Pa.

The bearing capacity of the beams reinforced with steel bars was calculated in similar manner and found to be *44.15 kN*, which is *17%* higher than experimental results.

5 Results and Discussion

Experimental as well as numerical deflections of the beams reinforced with BFRP bars were significantly greater than the deflections for beams reinforced with steel bars, that can be caused due to the significantly lower elasticity modulus of BFRP bars than that one for steel bars.

Additional aspect that demonstrate the convergence between experimental and numerical programmes was that in both studies the concrete regions were destroyed, rather than BFRP or steel bars. It is also observed that with an increase in tensile strength of concrete, the carrying capacity of the beam increases. That can be considered as one of the major aspects for estimation of the strength capacity of elements.

The difference between experimental and numerical outcomes for bearing capacity can be described by the presence of one or several factors. Initially, it can be explained by different bond characteristics between materials. Some scientific papers confirmed that FRP bar-to-concrete bond can be considered as competitive [14]. The test results obtained in [15] for FRP bars support that bond strength is proportional to the square root of the development length. The mechanism failure and high resistance to cyclic loadings can be interpret as important factor comparing with working of steel bars in this case. These issues indicates on the possibility to use BFRP bars in order to achieve balanced ratio, which is defined as the reinforcement ratio that simultaneously results in the rupture of the bars and crushing of concrete. Balanced ratio can be the reason of higher bearing capacity of the element.

Authors want to conclude, that for the investigation of a new materials, numerical modelling is insufficient and experimental work is a vital issue.

The authors wish to acknowledge the financial support of the project – “Innovative Hybrid - FRP composites for infrastructure design with high durability” NCBR: PBS3/A2/20/2015.

References

1. *ACI 440.4R-04: Prestressing Concrete Structures with FRP Tendons (Reapproved 2011), American Concrete Institute, the USA* (2011)
2. K. Protchenko, M. Wlodarchyk, E. Szmigiera, Proc. Eng. **111C**, 679-686 (2015)
3. A. Lapko, M. Urbanski, Materiały Budowlane **2013/3**, (2013)
4. M. Urbański, A. Łapko, Budownictwo i Architektura **13(3)**, 201-208 (2014)
5. B. Benmokrane, A.H. Ali, H.M. Mohamed, M. Robert, conference paper: 7th Intern. Conference on Advanced Comp. Materials in Bridges and Structures (2016)
6. K. Protchenko, J. Dobosz, M. Urbański, A. Garbacz, Journal of Civil Engineering, Environment and Architecture **XXXIII - 63**, 149-156 (2016)
7. N.M. Chikhradze, L.A. Japaridze, G.S. Abashidze, Composites and Their Applications, 221-246 (2012)
8. A. Dorigato, A. Pegoretti, Journal of Composite Materials **48**, 1121-1130 (2014)
9. R. Parnas, M. Shaw, Q. Liu, *Basalt Fiber Reinforced Polymer Composites* (Technical Report, Storrs, 2007)
10. R. Piekarski, Wydawnictwo Politechniki Częstochowskiej, Kompozyty **1(6)**, 26-31
11. E. Kormanikova, K. Kotrasova, Chem. Listy **105**, 758-762 (2011).
12. M. Abdel Gfahaar, A.A. Mazen, N.A. El-Mahallawy, Journal of Engineering Sciences, **34**, 227-236 (2006).
13. M. Urbanski, A. Lapko, A. Garbacz, Procedia Engineering **57**, 1183–1191, (2013)
14. A. Garbacz, M. Urbański, A. Łapko, Advanced Materials Research **1129**, 233-241, (2015)
15. C. P. Mosley, A. Koray Tureyen, R J. Frosch, ACI Structural Journal **105-S60**, 634-642 (2008).